

# Light trapping performance of the silicon nanowire and nanocone based solar cells

GUANG DAI<sup>a, b</sup>, RUOWU WU<sup>a</sup>, ANJUN ZHANG<sup>a, b</sup>, XUEJING BAO<sup>b</sup>, HONGPING ZHOU<sup>b</sup>, FEI SHEN<sup>b</sup>, ZHONGYI GUO<sup>b\*</sup>

<sup>a</sup> State Key Laboratory of Complex Electromagnetic Environment Effects on Electronics and Information System, Luoyang, 471003, China

<sup>b</sup> School of Computer and Information, Hefei University of Technology, Hefei, 230009, China

We have investigated the performances of the silicon nanowires (SiNW) and silicon nanocones (SiNC) arrays solar cell with different structural parameters. The structural parameters of the thin film solar cell, such as the filling ratio, the period and the length of the nano-wires/cones arrays, can affect the ultimate conversion efficiency greatly. For 3 $\mu\text{m}$  SiNW arrays solar cells, with or without the silicon substrates, the obtained corresponding optimizing ultimate efficiency reach to 24.07% and 21.99% respectively, and that of the SiNC arrays solar cells can reach to 31.39% nearly. We have also discussed the simulated results based on the multiple reflection effects, the graded refractive index theory, and guiding mode coupling effect, which will give a guideline for the optimal design of SiNW and SiNC based solar cells.

(Received May 15, 2015; accepted August 3, 2016)

**Keywords:** Solar Cell, Si Nanowire (SiNW), Si Nanocone (SiNC)

## 1. Introduction

In the past twenties years, nanostructured solar cells, such as nanoparticles [1-4], nanograting [5, 6], nanoporous [7-9] and nanowires [10-12], have attracted great attentions owing to their potential for enhancing the ability of light trapping effect, optical absorption, improving charge collection efficiency, enabling novel conversion mechanisms and using low-cost processes. Because the silicon nanowires (SiNWs) arrays could be fabricated into solar cell with radial p-n junction, it has been considered as the most effective way for enhancing the conversion efficiency (CE) of the solar cell significantly due to the feasibility of the directional separation between the light absorption and photo-generated carrier collection [13]. At the same time, the material cost of the solar cell can also be reduced effectively because it is possible to use Metallurgical grade silicon (MGS, ~99.99%) instead of crystal silicon (~99.9999%). SiNWs arrays can also suppress optical reflection and promote the trapping efficiency of incident photons effectively because of the multiple scattering effects and the enhanced light path in the samples. According to the theory of graded refractive index, SiNWs array can act as a buffer layer to intervene the difference in refractive indexes between air and a substrate [14]. Based on these distinct superiorities, therefore, in recent years, there are many groups focus on the researching topic of the SiNWs array solar cell, and the concrete CE of the SiNWs array solar cell reach to 12.8% nearly [14-16].

In this article, we have performed the numerical simulations by Finite-element-method (FEM) for investigating the optical characteristics of the SiNWs and

SiNCs based solar cell. Firstly, the total thickness of solar cell (Si wafer, SiNWs and SiNCs) are fixed into 3 $\mu\text{m}$ , then the optimal value of fill ratio (FR, defined as  $FR=d/P$ , where  $d$  and  $P$  are the diameter and the period of the SiNWs samples), optimized period and length of nanostructures could be obtained by simulation of determining the best ultimate conversion efficiency with the aids of real absorption in solar cell. For 3 $\mu\text{m}$  pure SiNWs (without the substrate), the optimizing ultimate conversion efficiency reaches to 21.99%, and for 3 $\mu\text{m}$  combined structures of SiNWs samples (0.8 $\mu\text{m}$  SiNWs and 2.2 $\mu\text{m}$  Si substrate), the optimizing ultimate efficiency reaches to 24.07%, however, for that of SiNCs samples, the optimizing ultimate efficiency reaches to 31.39% nearly, which agree well with the former experimental results because of the superior light trapping effect due to multiple reflection effects and the graded refractive index (GRI) effect.

## 2. Structure and simulation

Fig. 1 shows the schematic illustrations of the simulated solar cell structures respectively: (a) SiNWs array with substrate, (b) SiNWs array without substrate, (c) SiNCs with substrate. The corresponding electric field distributions in the wavelength of 977nm are also put at the right side of the schematic respectively. In our simulations, the incident light is normal to the Si substrate, that is to say the incident light is parallel to the Si nanowires (nanocones) arrays.

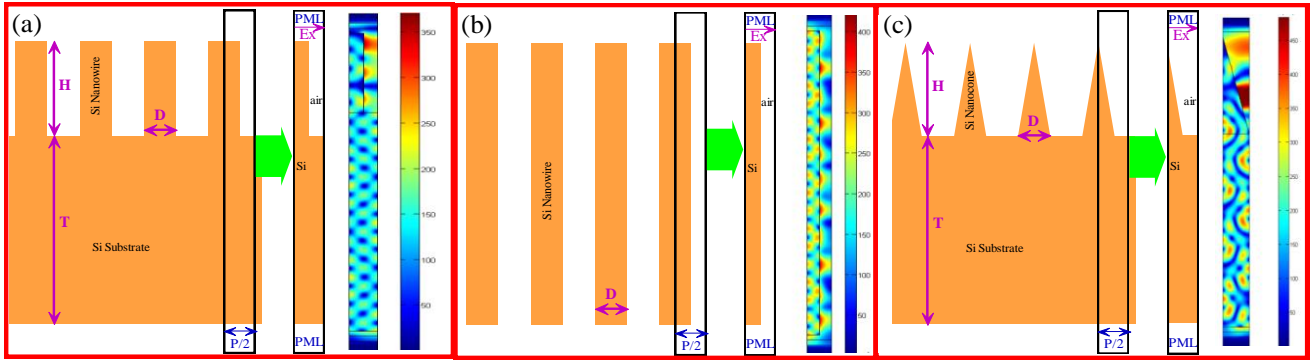


Fig. 1. Schematics of SiNWs arrays with substrate (a), SiNWs arrays without substrate (b), and SiNCs arrays with substrate (c). The corresponding electric field intensity distribution is shown in the right of the relative structures respectively.

The simulated nano-structures are periodic in  $x$  direction and we take the structure in the rectangle as a unit of the whole structure. By extending both of the units in  $x$  direction, the periodic SiNWs array and SiNCs array structures could be obtained. In our simulation, the optical field distribution, the concrete absorption and the conversion efficiency of the structured solar cell, could be obtained by Finite-element-method. Both of the PML layers are placed in the upper and bottom of the simulated region for avoiding the artificial boundaries' effects. A surface current is positioned in front of the structure as the incident light resource. The direction of the surface current is parallel to the  $x$  axis, indicating the direction of the E component of incident light. Considering the direction of propagation of the incident light, we know the incident wave is TM wave. As the structure is periodic and infinite along the  $x$  direction, PECs (perfect electric conditions) are applied at the edge of the geometrical cell, which can generate symmetric electric field. On PEC wall, there is no parallel component for electric field. So, if PECs are applied, the whole periodic geometry can be formed by mirroring the simulated area [17], as a result, only a half of a unit should be simulated. Here we use 2D geometrical structure, because this 2D approach enables a much simpler structure while yielding almost the same result with 3D approach. Firstly, the electromagnetic field distribution of the light waves at a certain position of nanostructures arrays is obtained by solving the Maxwell's equations and then reflectance  $R(\lambda)$ , and transmittance  $T(\lambda)$  can be detected by boundary probes. According to the equation:  $A(\lambda) = 1 - R(\lambda) - T(\lambda)$ , the concrete absorbance can be obtained easily. This is the brief overview of theory for our model. The optimized results can be obtained by changing the global parameters or the geometrical structure in our simulations. In order to quantify the absorption across the solar spectrum, we can calculate the ultimate efficiency. We assume that an incident photon which is absorbed can generate only one pair of electron and hole. And the concrete ultimate efficiency can be expressed by the following equation

[18]:

$$\eta = \frac{\int_{310}^{\lambda_g} I(\lambda) * A(\lambda) * \frac{\lambda}{\lambda_g} d\lambda}{\int_{310}^{4000} I(\lambda) d\lambda} \quad (1)$$

where  $\lambda_g$  represents the band gap of Si,  $I(\lambda)$  is the spectral irradiance of the AM1.5 reference spectrum in  $W/m^2/nm$ , and  $A(\lambda)$  is the absorbance mentioned above. According to the bandgap energy of crystalline silicon (1.1eV),  $\lambda_g = 1127nm$ . The lower limit (310nm) of integration corresponds to the energy of 4eV and the upper limit in denominator indicates the limit of data available for a solar spectrum. The short circuit current density can also be calculated to characterize the photoelectric conversion efficiency and it can be defined by the following equation:

$$J_{sc} = \frac{e}{hc} \int_{310nm}^{\lambda_g} \lambda I(\lambda) A(\lambda) d\lambda \quad (2)$$

where,  $h$  is the planck constant,  $c$  is the speed of the light and  $e$  is the electron charge,  $\lambda_g$  equals 1127nm corresponding to the band gap of Si.

### 3. Results and discussions

Fig. 2 shows the ultimate efficiencies of the SiNWs array with substrate as shown in Fig. 1 (a) with different filling ratio (FR) and the period (P). Here, the total depth (H+T) of the solar cell is fixed to 3000nm; the height (H) of nanowires arrays equals 800nm and the thickness of substrate (T) is 2200nm respectively. We calculate the ultimate efficiency and we identify that the best values for FR and period are 0.5 and 400nm respectively. The corresponding ultimate efficiency also reaches to 24.07% nearly. The corresponding short circuit current density of the optimized SiNWs reaches to 27.68mA/cm<sup>2</sup> nearly.

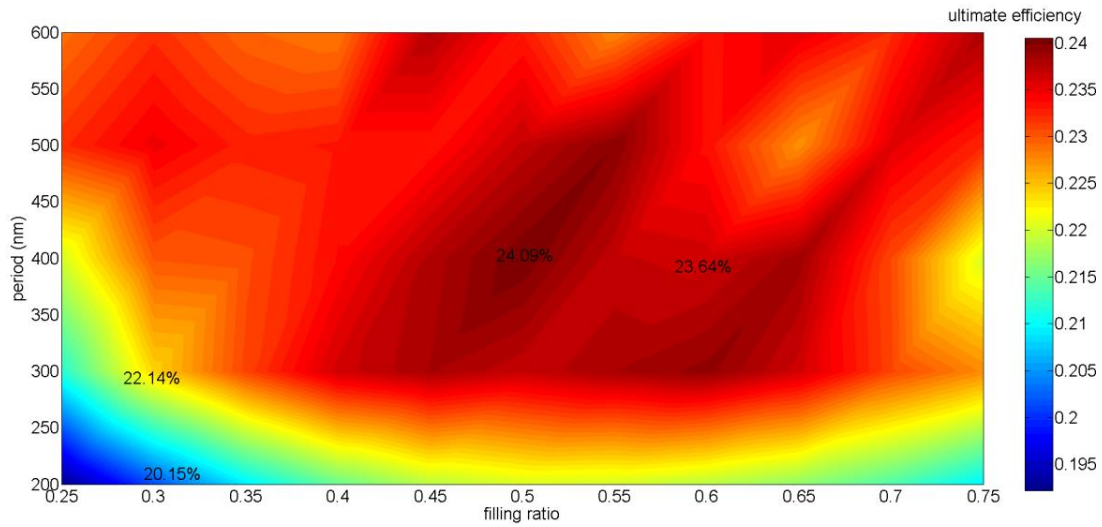


Fig. 2 The ultimate efficiency of thin film solar cell (SiNWs with silicon substrate ( $H=800\text{nm}$ ,  $T=2200\text{nm}$ ) as shown in Fig. 1 (a)) with different periods ( $P$ ) and filling ratios ( $FR$ ).

When  $P$  is less than  $600\text{nm}$ , the best value for  $FR$  varies from  $0.5$  to  $0.6$  as the variation of  $P$ . From the view of effective refractive index, the SiNW arrays can act as a buffer layer and can intervene the mismatch of refractive index happening at air-to-silicon substrate, which can result in the reduced reflection of the samples [4, 12]. When  $FR=0.5$ , the total reflection caused by mismatch of refractive index could be minimized. When  $FR \rightarrow 0$  or  $FR \rightarrow 1$ , the whole structure could be approximate to a planar solar cell without the nanostructures. So, when  $FR$  is too small or too large, the reflection would be higher. From the view of waveguide modes, a single nanowire can be regarded as a step-profile fiber, and the corresponding fiber parameter can be defined as  $V=2\pi p/\sqrt{n_{co}^2 - n_{cl}^2}$ . When  $V$  is less than  $2.405$ , there will be only fundamental mode ( $HE_{11}$  mode) in the SiNWs. The guide modes can be excited at specific wavelengths [19], and at these wavelengths, some part of the incident light can couple into the guide mode and propagate in the SiNWs, and the other part of the coupled light distributes in the surrounding air [20]. As the increase of diameter of the nanowire, multimodes could coexist in one nanowire [19], which leads to the reduction of reflection and field intensity enhancement in the nanowire. As a result, when  $FR$  is around  $0.5$  and  $P$  is larger than  $200\text{nm}$ , the diameters of nanowires are large enough so that the nanowires can couple some part of incident light into guide modes, which will prolong the optical path length of coupled incident and enhance the optical absorption and the ultimate efficiency. Because of these two physical mechanisms, the best value for  $FR$  varies from  $0.5$  to  $0.6$  as the variation of period. When  $P$  equals  $600\text{nm}$ , the best value for  $FR$  is  $0.75$ . We can see that the ultimate efficiency for  $P=600\text{nm}$  nanowires arrays decreases and then increases when  $FR$  is larger than  $0.45$ . For  $P=600\text{nm}$  nanowires arrays, the total reflection is the smallest when  $FR$  equals  $0.45$ . If the  $FR$  becomes larger, the total reflection will increase. However, the increase of  $FR$  will also cause the increase of guide mode coupling, which can enhance the absorption.

Therefore, as the period is large, the enhancement of absorption caused by guide mode coupling can compensate the reflection loss when  $FR$  equals  $0.75$ .

When  $P$  equals  $200\text{nm}$  or  $300\text{nm}$ , the ultimate efficiency increases until  $FR$  reaches the best value, and then, the ultimate efficiency will decrease as the increase of  $FR$ . However, when  $P$  is larger than  $300\text{nm}$  and  $FR$  is less than  $0.5$ , as the increase of  $FR$ , the ultimate efficiency increases and then decreases. These phenomena may be considered as the reflection from the air-to-NWs interface. When  $FR$  is relatively small, the mismatch of refractive index between the air and the nanowires arrays is small, which will reduce the reflection at the air-to-NWs interface. And also, when  $FR$  equals  $0.3$  or  $0.35$ , the diameter is large enough so that guide modes can coexist in one nanowire. By this way, the effective optical length of incident light can be prolonged, which will cause the increase of absorption and that of the ultimate efficiency. With the increase of the  $FR$ , more incident light can be coupled into the nanowires arrays and the reflection loss at the NWs-to-substrate becomes less, but the reflection loss at air-to-NWs interface also will be increasing, and the less reflection loss at the NWs-to-substrate cannot compensate the increase of reflection loss at the air-to-NWs interface, so the total reflection will be increase, and as a result, the ultimate efficiency will decrease. As the  $FR$  continues to increase, the total reflection reduces. More incident lights will be absorbed by the substrate, which can compensate the reflection loss in nanowires arrays.

We identify the best value for the period of  $P=400\text{nm}$  when  $FR$  reaches to the best value. From the viewpoint of wave optics, the 2D SiNWs can be regarded as 1D grating, the grating diffraction model can be applied to analysis our 2D SiNWs arrays, it can be described by the following equation [21]:

$$n_{\text{eff}} \sin(\theta_m) = n_i \sin(\theta_i) m\lambda \quad (3)$$

where  $p_0$  is the period of SiNWs,  $n_{\text{eff}}$  is the effective

refractive index of SiNWs,  $\theta_m$  is the diffraction angle,  $\theta_i$  and  $n_i$  equals 0 degree and 1 for normal incidence from the air. If  $p_0 n_{\text{eff}}$  is smaller than  $\lambda$ , only zeroth-order diffraction occurs which indicate that the diffracted light will still propagate in the direction of z-axis. As the increase of period,  $n_{\text{eff}} p_0$  can be larger than  $\lambda$  and higher-order diffraction may occur. The optical path can be prolonged by the diffraction. The diffracted light can also be coupled into Bloch mode in the SiNWs [22]. For the incident plane wave with wave vector  $\vec{k}$ , there are diffracted plane wave with all wave vector  $\vec{K}$ , possessing a lateral wave vector  $\vec{K}_{||} = \vec{k}_{||} + \vec{G}$ . Here,  $\vec{k}_{||}$  is the parallel-to-x axis component of incident wavevector and  $\vec{G}$  is a reciprocal lattice vector of the SiNWs photonic crystal. For zero-order diffraction,  $\vec{G}$  equals zero and the incident wave will propagate along y-direction. There are some bloch modes exist in SiNWs due to photonic band structure. These modes can be described as follows [23]:

$$u_{m,k_x,k_y} = \square_{m,k_x,k_y}(r) e^{-ik_x x} e^{-ik_y y} \quad (4)$$

where,  $\square_{m,k_x,k_y}(r)$  is a periodic function and has the same period with the SiNWs,  $e^{-ik_x x}$  and  $e^{-ik_y y}$  express the phase factors in the x, y-direction respectively. The incident plane wave can couple into the bloch mode with the same lateral vector at the same frequency inside photonic crystals. After the momentum match and mode excitation, the coupled plane wave can propagate inside photonic crystal with nonzero lateral wave vector. By this way, the optical path can be further enhanced. Total internal reflection can also make a contribution to light

trapping when nonzero order diffraction occurs. The critical angle for total internal reflection satisfy the following equation:

$$n_{\text{eff}} \sin(\theta_c) = 1 \quad (5)$$

When  $\theta_m$  is larger than  $\theta_c$ , total internal reflection will occur at the SiNWs/air interface and the diffracted light can be trapped in the solar cell, which can also make a contribution to light harvesting[21].

From the aspect of the coupling to the waveguide modes, if the diameters of nanowires are too small, the guide mode coupling is relatively weak because there is only one guide mode in the SiNW. As a result, the ultimate efficiency will be low. As the increase of period, the diameters become larger. Consequently, if the diameter is large enough, waveguide modes can coexist in one nanowire and the incident light can be coupled into these waveguide modes, which leads to the reduction of reflection and the increase of light confinement in the nanowire. From these two viewpoints, we can obtain that the ultimate efficiency may increase at first as the increase of period. What is more, according to the grating diffraction equation, the diffraction angle will decrease when period increase when diffraction orders are fixed. The diffraction angle of 1st order diffraction may be smaller than critical angle, which leads to mode leakage [24]. Consequently, the nanowires arrays yield lower ultimate efficiency when period equals 500nm or 600nm. Therefore, in our simulation, we choose  $P=400\text{nm}$ ,  $FR=0.5$  to be the best parameters.

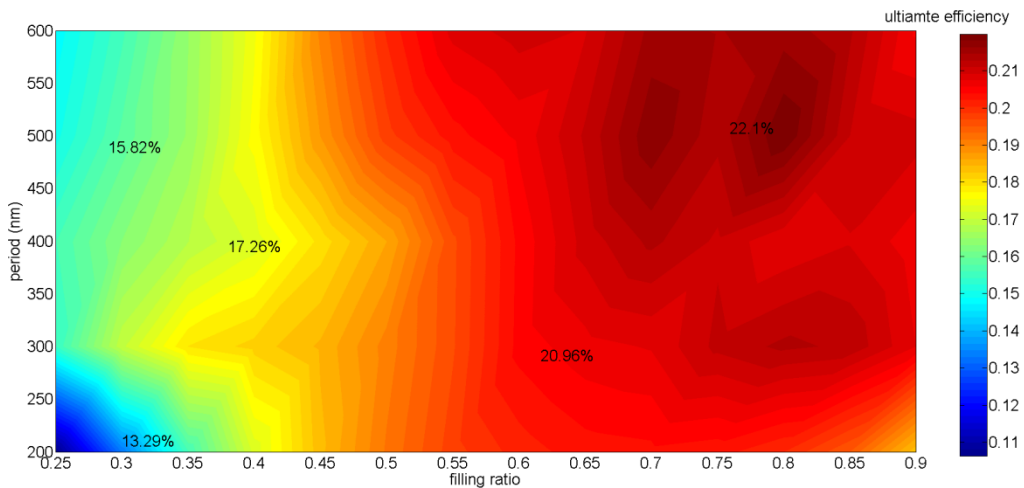


Fig. 3 The ultimate efficiency of the Si solar cell (SiNWs without silicon substrate as shown in Fig. 1 (b)) with different FRs and periods.

We have also searched for the best values of both FR and period of P for SiNWs arrays without substrate as shown in Fig. 1 (b). In order to compare with the SiNWs arrays with substrate as depicted in Fig. 1 (a), the length of SiNWs is also fixed at 3000nm. Fig. 3 shows the ultimate efficiency of SiNWs arrays solar cell without substrate as the function of FR and period. We identify that the best

parameters for FR and period are 0.8 and 500nm respectively. The corresponding ultimate efficiency and short circuit current density can reach to 21.99% and  $25.28\text{mA/cm}^2$  respectively. .

Obviously, if the FR is low, the ultimate efficiency must be low because the transmittance will be quite high. As the increase of FR, more incident lights will interact

with the SiNWs arrays and the transmittance will become less and less. And also, as the increase of the FR, more incident lights can be coupled into guide modes, which would result in the enhancement of ultimate efficiency. Because of the absence of substrate, the FR should be large enough to reduce the loss of transmission. However, the larger FR would cause a larger reflectance. In extreme condition, if FR equals 1, the whole structure can be

regarded as a planar solar cell. So, there must be an upper limit for FR and according to the simulated result, the value for the upper limit varies from 0.7 to 0.8. As the increase of period, some waveguide modes may coexist in one SiNW. Incident light can be coupled into these guide modes and propagate in the nanowire, which will enhance the absorptance greatly.

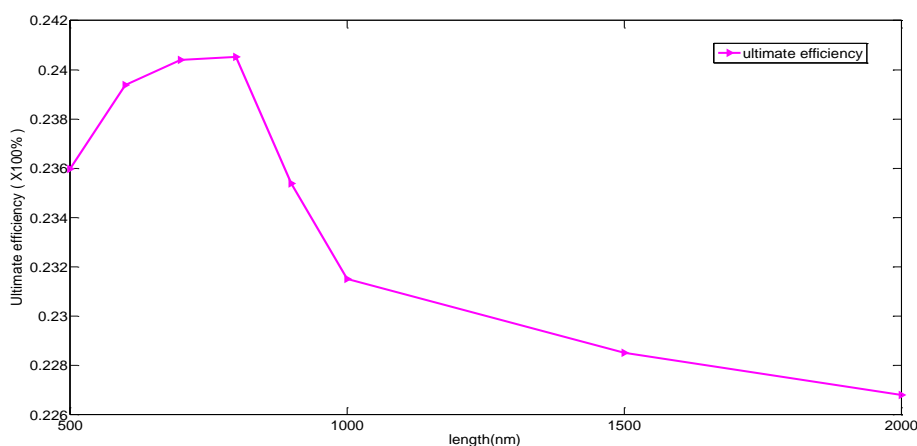


Fig. 4. The ultimate efficiency of SiNWs solar cell as a function of the length of nanowires.

As you can see in Fig. 3, with the absence of substrate, the maximum value for the ultimate efficiency of nanowires arrays is 21.99%. This value is lower than that of nanowires arrays with substrate, therefore, the substrate is essential for the light harvesting. However, if the total thickness of the sample ( $H$  (height of nanowires)+ $T$  (thickness of substrate)) is set to be 3000nm, we should find a best value for thickness of substrate ( $T$ ) and the height of nanowires ( $H$ ) respectively. Here, the FR and period is set to be 0.5 and 400nm respectively, and eight lengths of nanowires (500nm, 600nm, 700nm, 800nm, 900nm, 1000nm, 1500nm and 2000nm) are chosen in our simulation. Fig. 4 shows the ultimate efficiency of nanowires arrays as a function of the length ( $H$ ) of nanowires, and the best value of the length of nanowires can be determined as 700nm or 800nm, which corresponds to the optimized ultimate efficiency of 24.05%. As depicted in Fig. 4, when the length of nanowires is larger than 800nm, we can see that the longer the SiNW is, the lower the ultimate efficiency is. Because when the length of nanowires is larger than 700nm, the nanowires are long enough to absorb the incident shorter wavelength light sufficiently. However, some of the incident longer wavelength light may not interact with nanowires effectively and finally penetrate through the nanowires arrays. Because with the increase of the length of SiNWs, the substrate would become thinner, and the optical path length for this part of incident longer wavelength light will become shorter which is not sufficient for absorbing this part of incident light absolutely. On the other hand, the length of the nanowires should not be too short. If the nanowires are too short, the incident light which interacts

with them will not be absorbed sufficiently and it will be reflected by the silicon substrate. Therefore, we identify 800nm to be the best value for the length of nanowires in our simulation model.

In order to collect the photon-generated carriers effectively, for achieving higher conversion efficiency, silver thin film can be exploited to be the bottom electrode, which can also be used as the back-reflector for reflecting the incident light which is not absorbed by the nanowires arrays. Fig. 5(a) illustrates the ultimate efficiency of nanowires arrays solar cell with Ag back reflector as the function of filling ratio and period. The highest value of ultimate efficiency of 25.8% is achieved at  $a=600$ , and the filling ratio is 0.75, which is higher than that of structures comprised of Si nanowires and Si substrate. The corresponding short circuit current density is  $31.22\text{mA}/\text{cm}^2$ . This enhancement of the ultimate efficiency can be firstly attributed to the back-reflecting effect in longer wavelength region. The longer wavelength light that can't be absorbed efficiently will be reflected into the SiNWs array again by the bottom electrode, which will enhance the absorption. There will also be the excitation of surface plasmonic polaritons (SPPs) at the surface of Ag contacted to Si or air, because the phase match condition can be fulfilled due to the period of nanowires arrays, which can be verified by our simulating results as shown in Fig. 5 (b) where the distribution of electric field intensity at the interface between the nanowires arrays and Ag thin-film indicates that the SPPs can be excited and propagate along the Si-Ag interface. The reemission of these surface plasmonics wave can also enhance the absorption of the SiNWs effectively [19].

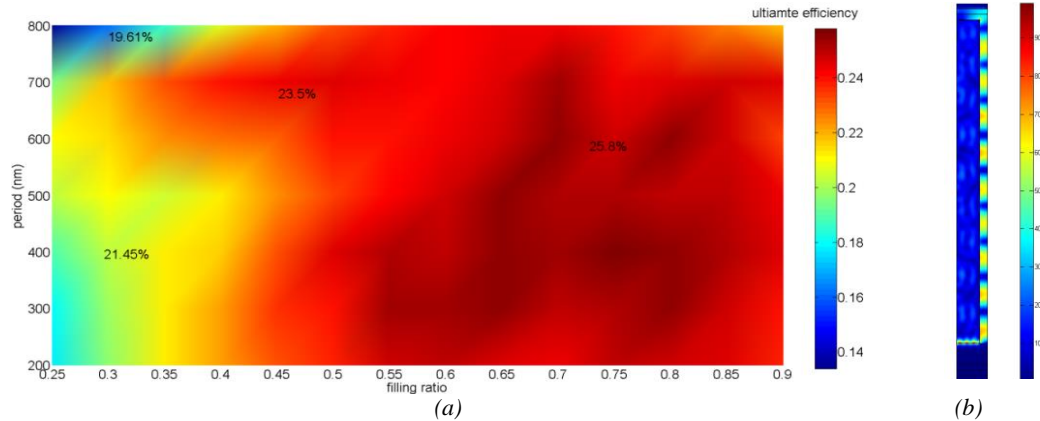


Fig. 5 (a) The ultimate efficiency of SiNWs solar cell with Ag reflector as the function of period and filling ratio. (b) The intensity distribution in the SiNW at the wavelength of 741nm, we can observe the existence of SPPs in the interface between the nanowire arrays and Ag thin-film. .

For the structures of nanocones, we just consider the nanocones with silicon substrate, as shown in Fig.1(c). The diameters of nanocones changes gradually along the direction of the radius of the nanocones. Thus, the effective refractive index of nanocones arrays changes gradually along z direction, which will result in a lower reflection loss at the air-arrays interface or in the nanocones arrays region. The reflection loss mainly take place at the arrays-substrate interface, which is caused by the refractive index mismatch between the nanocones arrays and the substrate. Here, FR defined as  $D(z=0)/a$ , where  $D(z=0)$  is the diameter of nanocones at the arrays-substrate interface. Consequently, as the increase of FR, the refractive index mismatch between nanocones arrays and the substrate becomes less and less, which would lead to the decrease of reflection loss. Therefore, we can obtain that the best FR is 1 for nanocones.

Fig. 6 shows the ultimate efficiency of nanocones solar cell as a function of period (varying from 300nm to 800nm). The height (H) of the nanocones and the depth of the silicon substrate are set into 1000nm and 2000nm respectively. From Fig. 6, we can obtain that the optimal period is 600nm. The SiNCs can be regarded as grating too and the analysis for SiNWs can also make sense in SiNCs array. And the nanocones can also couple incident light into waveguide modes. As P becomes larger, more incident light can be coupled into waveguide modes, which causes the enhancement of ultimate efficiency. As a result, when  $P < 600$ nm, the ultimate efficiency increase as the increase of period. However, when P is larger than 600nm, although the guide modes can enhance the absorption compared to that of  $P=600$ nm, from equation (2) we can obtain that if the diffraction order is fixed, the diffraction angle decrease as the increase of period, which will cause the reduced optical path length and the reduced absorption. In this way, the absorption enhancement caused by guide mode coupling cannot compensate the loss of transmission because of the larger periods of SiNCs. As a result,  $a=600$ nm is the optimal value for period, and the corresponding ultimate efficiency is 31.39%. The short circuit current density of  $P=600$ nm SiNCs can reach to  $36.46\text{mA}/\text{cm}^2$ .

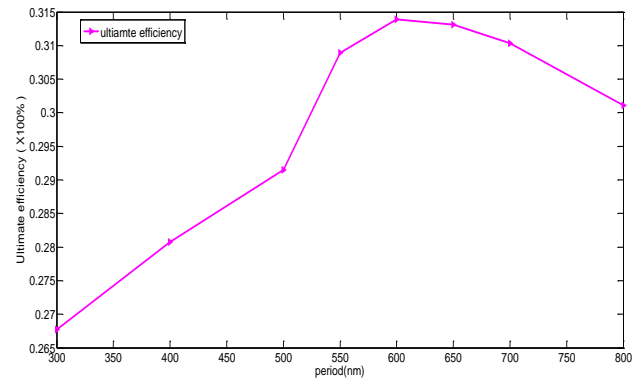


Fig. 6. The ultimate efficiency of SiNCs solar cell as a function of period. .

We have also investigated an optimized length for nanocones when the total thickness of the sample (H (height of nanocones)+T (thickness of substrate)) is fixed to be 3000nm, in which FR and the period are fixed to be 1 and 600nm respectively. Fig.7 shows the ultimate efficiency as a function of the height of nanocones. We calculate the ultimate efficiency and obtain that the best value for the length of nanocones is 1000nm. The corresponding ultimate efficiency is 31.39%. According to the theory of effective refractive index, in this case, the effective refractive index will change more gradually with increasing height of nanocones. If the height of nanocones is enlarged, the reflection loss in nanocones region will be reduced. However, the increasing height of the nanocone leads to the decrease of the thickness of the substrate. The optical path of the incident light with longer wavelengths would be shortened, and the absorption for this part of light would be decreased correspondingly. Due to the tradeoff of these two physical mechanisms, the best value for the length of nanocones is 1000nm when the thickness of Si wafer is fixed to be 3000nm. We can see that the maximum value for ultimate efficiency of Si nanowires arrays solar cells is 24.05%, but that of Si nanocones arrays solar cells reaches to 31.39%. The performance of Si nanocones arrays is better, because the reflectance of nanocones arrays is much lower than that of nanowires arrays due to the graded refractive index of nanocones arrays.

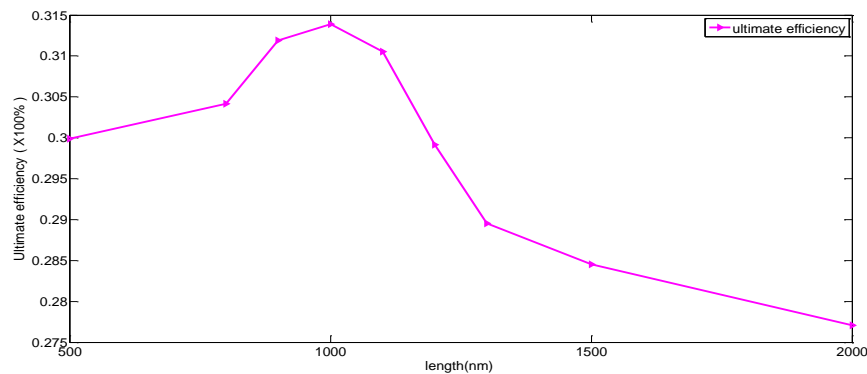


Fig. 7. The Ultimate efficiency of SiNCs solar cell as a function of the length of the SiNCs.

#### 4. Summary

In this work, we have investigated the optical performance of SiNW and SiNC based solar cell and searched for the best structural parameters for these structures. According to our simulation results, the structure parameters such as filling ratio, period and the length of the structure have great influence on the ultimate efficiency. In our simulation, for  $3\mu\text{m}$  SiNW arrays solar cells, with or without the silicon substrates, the obtained corresponding optimizing ultimate efficiency reach to 24.07% and 21.99% respectively, and that of the SiNC arrays solar cells can reach to 31.39% nearly. We discussed the optimal parameters from the view points of wave guide mode coupling, grating diffraction, mutireflection, and the graded refractive index theory. This work can serve as a guideline for the designing of SiNW and SiNC based solar cells.

#### Acknowledgements

The authors gratefully acknowledge the financial supports for this work from the funding of State Key Laboratory of CEMEE (CEMEE20160101B), the National Natural Science Foundation of China under Grant No. 61575060, and the Fundamental Research Funds for the Central Universities (2015HGCH0010).

#### Reference

- [1] C. Pahud, O. Isabella, A. Naqavi, F. J. Haug, M. Zeman, H. P. Herzig, Ch. Ballif, *Opt. Express* **21**, A786 (2013).
- [2] H. Tan, R. Santbergen, A. Smets, M. Zeman, *Nano Lett.* **12**, 4070 (2012).
- [3] Sonali Das, Avra Kundu Hiranmay Saha, Swapan K. Datta, *Journal of Modern Optics*, **60**, 556 (2013).
- [4] Bao-zeng Li, Xiao-xiao Su, Jing-quan Lin, Xun Gao, Jian-guo Lei, Hai-yan Tao, *Journal of Modern Optics*, **58**, 796 (2011).
- [5] N. Huu, M. Cada, J. Pistora, *Opt. Express* **22**, A68 (2014).
- [6] Rana Biswas, Erik Timmons, *Opt. Express* **21**, A481 (2013).
- [7] S. E. Han, G. Chen, *Nano Lett* **10**, 1012 (2010).
- [8] Qing Guo Du, Chan Hin Kam, Hilmi Volkan Demir, Hong Yu Yu, Xiao Wei Sun, *Opt. Lett.* **36**, 1713 (2011).
- [9] Wei Wang, Jiasen Zhang, Yu Zhang, Ziang Xie, Guogang Qin, *J. Phys. D: Appl. Phys.* **46**, 195106 (2013).
- [10] E. Garnett, Peidong Yang, *Nano Lett* **10**, 1082 (2010).
- [11] Chenxi Lin, Michelle L. Povinelli, *Opt Express* **17**, 19371 (2009).
- [12] Kui-Qing Peng, Shuit-Tong Lee, *Advanced Materials* **23**, 198 (2011).
- [13] J. Y. Jung, Zhongyi Guo, S. W. Jee, H. D. Um, K.T. Park, M. S. Hyun, J. M. Yang, J. H. Lee, *Nanotechnology* **21**, 455303 (2010).
- [14] Jin-Young Jung, Zhongyi Guo, Sang-Won Jee, Han-Don Um, Kwang-Tae Park, Jung-Ho Lee, *Opt Express* **18**, A286 (2010).
- [15] K. T. Park, Zhongyi Guo, H. D. Um, J. Y. Jung, J. M. Yang, S. K. Lim, Y. S. Kim, J. H. Lee, *Opt. Express* **19**, A41 (2010).
- [16] H. Um, K. Park T, J. Jung, X. Li, K. Zhou, S. Jee, J. Lee, Incorporation of a self-aligned selective emitter to realize highly efficient, *Nanoscale* **6**, 5193 (2014).
- [17] J. Kupec, B. Witzigmann, *J. Comput. Electron.* **11**, 153 (2012).
- [18] Keya Zhou, Sang-Won Jee, Zhongyi Guo, Shutian Liu, Jung-Ho Lee, *Appl. Optics* **50**, G63 (2011).
- [19] Keya Zhou, Zhongyi Guo, Xiaopeng Li, J. Y. Jung, S. W. Jee, K. T. Park, H. D. Um, Ning Wang, J. H. Lee, *Opt Express* **20**, A777 (2012).
- [20] K. Seo, M. Wober, P. Steinvurzel, E. Schonbrun, Yaping Dan, T. Ellenbogen, Kenneth B. Crozier, *Nano Lett* **11**, 1851 (2011).
- [21] R. Y. Zhang, B. Shao, J. R. Dong, J. C. Zhang, H. Yang, *J. Appl. Phys.* **110**, 113105 (2011).
- [22] Alongkarn Chutinan, Sajeev John, *Phys. Rev. A* **78**, 023825 (2008).
- [23] Bjorn C. P. Sturmberg, Kokou B. Dossou, Lindsay C. Botten, Ara A. Asatryan, Christopher G. Poulton, C. Martijn de Sterke, Ross C. McPhedran, *Opt. Express* **19**, A1067 (2011).
- [24] Peihua Wangyang, Qingkang Wang, Kexiang Hu, Xia Wan, Kun Huang, *Optics Communications* **294**, 395 (2013).

\*Corresponding author: guozhongyi@hfut.edu.cn